UDC 621.313.318 https://doi.org/10.20998/2074-272X.2025.3.01

V.F. Bolyukh

# Electromechanical processes during the start of induction-type magnetic levitation

***Purpose.*** *A study of induction-type magnetic levitation by determining the electromechanical processes that occur when a stationary inductor is connected to an alternating voltage source and the levitation of an anchor made in the form of a multi-turn short-circuited winding with an attached load.* ***Methodology.*** *Using a mathematical model describing an inductor and an anchor with concentrated parameters, solutions are presented for equations describing the interconnected electrical, magnetic, mechanical and thermal processes that occur in induction-type magnetic levitation.* ***Results.*** *The influence of the frequency of the alternating current source on the electromechanical processes of levitation, which occur at different parameters of the anchor, is established. Due to the phase delay of the induced anchor current in relation to the inductor current, an electrodynamic force directed downwards arises at certain moments of their period. The total force acting on the anchor, due to the electrodynamic component, is of an alternating nature with a predominance of the positive, upwardly directed component, which causes pulsations of the anchor speed.* ***Originality.*** *The force acting on the anchor due to the electrodynamic component is of an alternating nature with the positive component directed upwards dominating. The resulting oscillatory damping mechanical process occurs with an increase in the oscillation period and a decrease in its amplitude.* ***Practical value.*** *It has been established that the maximum value of the lifting force acting on the anchor is achieved at an alternating current frequency in the range from 75 to 125 Hz, and the highest value of the steady-state levitation height is realized for an anchor similar to an inductor at a frequency of 75 Hz.* References 37, figures 6.

*Key words:* **magnetic levitation of induction type, mathematical model, experimental test, starting electromechanical characteristics, oscillatory electromechanical process.**

***Мета.*** *Дослідження магнітної левітації індукційного типу шляхом визначення електромеханічних процесів, що виникають при підключенні нерухомого індуктора до джерела змінної напруги та левітації якоря виконаного у вигляді багатовиткової короткозамкненої обмотки з приєднаним навантаженням.* ***Методологія.*** *За допомогою математичної моделі, яка описує індуктор та якір із зосередженими параметрами, представлені рішення рівнянь, що описують взаємопов'язані електричні, магнітні, механічні та теплові процеси, що виникають у магнітній левітації індукційного типу.* ***Результати.*** *Встановлено вплив частоти джерела змінного струму на електромеханічні процеси левітації, що виникають за різних параметрів якоря. Через фазову затримку індукованого струму якоря по відношенню до струму індуктора в певні моменти їх періоду виникає електродинамічна сила спрямована вниз. Сумарна сила, що діє на якір, через електродинамічний складник, носить знакозмінний характер з переважанням позитивної, спрямованої вгору складової, що обумовлює пульсації швидкості якоря.* ***Оригінальність.*** *Діюча на якір сила через електродинамічну складову носить знакозмінний характер з переважанням позитивної, спрямованої вгору складової. Виникаючий при цьому коливально загасаючий механічний процес відбувається зі збільшенням періоду коливань та зменшенням його амплітуди.* ***Практична цінність.*** *Встановлено, що максимальна підйомна сила, що діє на якір, досягається при частоті змінного струму в діапазоні від 75 до 125 Гц, а найбільша висота левітації, що встановилася, реалізується для якоря, аналогічного індуктору, при частоті 75 Гц.* Бібл. 37, рис. 6.

*Ключові слова:* **магнітна левітація індукційного типу, математична модель, експериментальне випробування, пускові електромеханічні характеристики, коливальний електромеханічний процес.**

**Introduction.** Magnetic levitation allows for qualitative improvement of existing technologies and finds application in transport, aerospace, chemical, biomedical engineering and other fields of science and technology. High-speed trains have been created on the basis of magnetic levitation and contactless suspension of aircraft models in wind tunnels is provided [1]. It helps circulate blood in the human chest, is used in the production of integrated circuits, measures dimensions with subatomic resolution, is involved in plasma research, melts and mixes chemically active high-temperature metals, simulates the sense of touch in tactile systems, cools laptops, enriches uranium and isotopes in centrifuges, stores energy in rotating flywheels, and powers rotors in machines [2]. Levitating micro-actuators eliminate the mechanical connection between fixed and moving parts, ensuring that inertial forces dominate over frictional forces [3]. Based on magnetic levitation, electromagnetic energy sources driven by motion are being developed, which are used for autonomous power supply of various high-tech devices, such as remote sensors, wearable devices, biomedical implants, etc. [4].

**Features of the application of magnetic levitation.** Magnetic levitation is used in actuators, accelerometers, gyroscopes, magnetic bearings, dampers, etc. It is used to stabilize and control sea vessels, spacecraft, and other critical objects.

In micro-drives, magnetic levitation not only eliminates friction, but also essentially creates a built-in micro-sensor with a long service life [3]. Levitating micro-actuators can operate in harsh conditions (with increased vibration and temperature, in a chemically aggressive environment, etc.), preventing contact of the micro-object with surfaces. They are used as sensors, motors, switches, accelerators, particle traps, conveyors, bearings, etc.) [3]. The micro-actuator allows for the implementation of a combination of induction-type magnetic levitation and an electrostatic actuator [5]. The mathematical model of the said levitation considers a conducting disk located between two circular currents. Such a model takes into account two degrees of freedom, allowing for the evaluation of static displacement and suspension stability.

Magnetic levitation is used to stabilize and stabilize a vessel, to reduce vibration and noise [6]. For these purposes, the accelerations of the stator and the stabilizing mass block were measured when the excitation winding was supplied with a sinusoidal voltage of 0–500 Hz.

The contactless magnetically stabilized spacecraft provides increased reliability and more precise control in a six-degree-of-freedom system [7]. Control of the excitation current of the contactless ring electromagnetic drive directly affects its orientation characteristics. Magnetic

bearings are used for the inertial drive of the spacecraft, and active control is used to eliminate unbalanced vibration in the magnetic levitation system [8].

The dual-hinged gyroscope of the magnetic levitation spacecraft provides position determination and position control [9]. The dual-axis angular velocity of the spacecraft is determined from control signals in the active magnetic suspension control system for the high-speed rotor. The angular velocity of the magnetic levitation gyroscope is measured by determining the current and noise of the tilt signal on the orientation accuracy of the spacecraft [10].

Magnetic levitation is used for magnetic bearings and dampers because they are stable and easy to use at both low and medium speeds. The magnetic damper reduces vibrations and noise in devices [11], and the active magnetic bearing suppresses disturbances in the control system and displacement vibrations [12].

The three-magnetic bearing platform provides drive weight compensation with ultra-precise installation, long stroke and high acceleration [13]. It uses magnetic bearings to provide lifting force and in-plane torque. Magnetic levitation can be effectively used in high-precision gravimeters to reduce autoseismic vibrations [14, 15].

A miniature rotating gyroscope is described in [16] in which a 0.5 mm thick aluminum rotor levitates and rotates relative to a flat coil. When high-frequency alternating current with temporal and spatial phase distribution is applied to the coil, the rotor rotates. Two internal conductors provide levitation, and the outer conductor provides lateral stability, preventing the rotor from sliding sideways. When tested for 200 hours, the micromotors remained operational at high current densities and elevated temperatures, showing no signs of degradation.

A promising direction of magnetic levitation is medicine. For a disposable extracorporeal system, a magnetically levitating centrifugal pump has been developed that provides blood circulation [17]. Such a pump, with high productivity, eliminates mechanical contact with the impeller, reduces heating and reduces blood trauma, preventing the formation of blood clots.

However, in a magnetic levitation system there is a problem of stabilizing suspended bodies. The stability of the system is affected by the mechanical interface between the levitation object and the loaded device, and self-exciting vibration occurs during operation. To study the effect of the gap size on the mechanical behavior of the system, a coupled electromagnetic-mechanical model with lumped parameters was considered in [18]. It was found that with a decrease in the gap size, the vibration frequency increases.

In [19], the dynamic electromagnetic characteristics of an electrodynamic levitation system with permanent magnets are investigated. The test setup is used to determine the speed characteristics, lateral stability and vertical vibration. A massive object is suspended in the air at a height of 30 mm [20]. Levitation can also be realized with a small gap, for example, at a distance of up to 5 mm between two ferromagnetic cores [21].

Of particular interest is magnetic levitation of the induction type (MLIT), which does not require either permanent or superconducting magnets. In it, the height of the suspension of the conductive anchor can be easily changed by regulating the alternating current feeding the inductor. Such levitation can be implemented in various devices in the presence of an electrically conductive element that is subject to an alternating or series of magnetic field pulses [22, 23].

In the work [24] an electromechanical model of the MLIT of a conductive anchor in the form of a ring is constructed and investigated. The equilibrium positions of the levitating ring are determined, the stability is investigated and an expression for the rigidity of the suspension is obtained.

To stabilize the MLIT, a magnetic resonance connection is used between a stationary inductor and a levitating multi-turn anchor [25]. To calculate such a suspension, analytical solutions of equivalent circuits were used, on the basis of which the currents in the inductor and anchor, forces relative to the gap size and the applied frequency of the alternating voltage were considered. Experimental and theoretical results show that positive rigidity is possible, which is necessary for self-stabilization of the magnetic suspension.

The MLIT allows energy to be transferred to a levitated object even if there is a large gap between the inductor and the anchor. Magnetically coupled circuits have two resonant frequencies, the attractive force is generated at a lower resonant frequency, and the repulsive force is generated at a higher resonant frequency [25]. The damping characteristics and the rigidity of the suspension depend on the size of the gap, the amplitude and frequency of the alternating voltage source.

One of the effective MLIT devices is the Thomson's Jumping Ring, which consists of a fixed inductor in the form of a multi-turn coil and a vertically located ferromagnetic core in the form of a steel rod that protrudes beyond the upper limit of the coil [26]. When alternating current is applied to the inductor, the conductive anchor, in the form of a thin ring placed on a ferromagnetic core, jumps to a certain height, after which it is held in a state of levitation relative to the coil. The Thomson apparatus was used to measure the phase delay of the current and force in the frequency range of 20–900 Hz [27]. Stroboscopic photographs of the jumping ring at room temperature and at liquid nitrogen temperature show that the jump height is determined by the time-averaged mechanism of the inductive phase delay. The stack of thin rings levitates at a higher altitude than a single ring because the inductive phase delay begins to dominate the parallel resistance of the combined rings.

Based on the analytical model of Thomson's apparatus, the dependences of the force acting on the ring on the phase, amplitude and frequency of the exciting current were established [28]. The theory of an ideal alternating current transformer is also used to calculate the parameters [29]. The electrodynamics of a levitating ring demonstrates a changing mutual inductance between the ring and the coil [30].

The dependences of the jump height of the ring on its material (copper and aluminum alloys), mass, temperature, and the number of rings of different heights were obtained [31]. The jump height increases and shifts to a lower optimal mass when the rings are cooled to a

temperature of 77 K. The throwing heights of brass, copper, and aluminum rings at room and nitrogen temperatures and different applied voltages were studied [32]. Synchronization of two rings of the Thomson apparatus, powered by alternating current, has found application in mobile robotics [2].

However, the existing Thomson devices implementing MLIT contain a ferromagnetic core protruding beyond the coil surface, which affects the design of the suspended object and introduces nonlinearity into the levitation process control system. Thomson devices were mainly used to study and demonstrate the effect of magnetic levitation without a load, and were not considered as a power suspension. This can also explain the design of the conductive anchor in the form of a ring, which is not advisable when feeding the inductor with high-frequency current. The height of the ring toss is mainly analyzed, while in the practical implementation of magnetic levitation, the size of the gap between the hovering anchor and the stator inductor and the time of the steady-state process are important.

**The aim** of the article is to study magnetic levitation of the induction type by determining the electromechanical processes that occur when a stationary inductor is connected to a source of alternating voltage and the levitation of an anchor made in the form of a multi-turn short-circuited winding with an attached load.

**Mathematical model of MLIT.** Let us consider electromechanical processes in a one-dimensional MLIT, in which a fixed inductor is connected to a high-frequency voltage source, and a coaxially mounted conductive anchor can move along only one spatial coordinate. The anchor is made in the form of a multi-turn short-circuited winding on which a load (an object being lifted) is installed. In this case, if the anchor is wound with a relatively thin wire, it is possible to analyze the influence of its height on the operation of MLIT, neglecting the skin effect.

We will assume a strictly vertical movement of the anchor along the $z$ axis relative to the stationary inductor. Let us consider a mathematical model of MLIT, in which the magnetic connection between the inductor and anchor changes. To describe MLIT processes, we will use electric circuits with concentrated parameters of the inductor and anchor, the active resistances of which depend on their heating temperature [33].

Note that when magnetic levitation is started, the temperature of the active elements may not increase significantly, but in a steady state this temperature can significantly affect the nature of electromechanical processes. Therefore, we will consider a universal mathematical model that describes processes in different operating modes.

To take into account the interconnected electrical, magnetic, mechanical and thermal processes, we will present the solutions of the equations describing these processes in a recurrent form [34]. Electrical processes in the active elements of the MLIT (inductor and anchor) can be described by a system of equations:

$$R_1(T_1)i_1 + L_1\frac{\mathrm{d}i_1}{\mathrm{d}t} + M(z)\frac{\mathrm{d}i_2}{\mathrm{d}t} + i_2 v_z(t)\frac{\mathrm{d}M}{\mathrm{d}z} = u(t), \quad (1)$$

$$R_2(T_2)i_2 + L_2\frac{\mathrm{d}i_2}{\mathrm{d}t} + M(z)\frac{\mathrm{d}i_1}{\mathrm{d}t} + i_1 v_z(t)\frac{\mathrm{d}M}{\mathrm{d}z} = 0, \quad (2)$$

where $n$ = 1, 2 are the indices of the inductor and anchor, respectively; $M(z)$ is the mutual inductance between the active elements; $v_z$ is the velocity of the anchor along the $z$ axis; $u(t) = U_m\sin(\omega t + \psi_u)$ is the voltage of the power source; $i_n$, $R_n$, $L_n$, $T_n$ are the current, active resistance, inductance and temperature of the $n$-th active element, respectively.

Using the relationships from work [35], the following expressions can be written for the currents of the active elements of the MLIT:

$$i_1(t_{k+1}) = -\frac{i_2(t_k)v_z(t_k)}{R_1}\frac{\mathrm{d}M}{\mathrm{d}z} + \Big(u(t_k) - R_1 i_1(t_k) - i_2(t_k)v_z(t_k)\times$$
$$\times\frac{\mathrm{d}M}{\mathrm{d}z}\Big)\frac{\alpha_1\exp(\alpha_2\Delta t) - \alpha_2\exp(\alpha_1\Delta t)}{R_1(\alpha_2-\alpha_1)} + \frac{u(t_k)}{R_1} +$$
$$+\frac{\exp(\alpha_2\Delta t) - \exp(\alpha_1\Delta t)}{(\alpha_2-\alpha_1)(L_1L_2 - M^2)}\Big\{u(t_k)L_2 + \Big[v_z(t_k)M\frac{\mathrm{d}M}{\mathrm{d}z} - R_1L_2\Big]\times$$
$$\times i_1(t_k) + \Big[R_2M - v_z(t_k)L_2\frac{\mathrm{d}M}{\mathrm{d}z}\Big]i_2(t_k)\Big\}; \quad (3)$$

$$i_2(t_{k+1}) = -\frac{i_1(t_k)v_z(t_k)}{R_2}\frac{\mathrm{d}M}{\mathrm{d}z} + \Big[i_2(t_k) + \frac{i_1(t_k)v_z(t_k)}{R_2}\frac{\mathrm{d}M}{\mathrm{d}z}\Big]\times$$
$$\times\frac{\alpha_2\exp(\alpha_1\Delta t) - \alpha_1\exp(\alpha_2\Delta t)}{\alpha_2-\alpha_1} + \frac{\exp(\alpha_2\Delta t) - \exp(\alpha_1\Delta t)}{(\alpha_2-\alpha_1)(L_1L_2 - M^2)}\times$$
$$\times\Big\{i_1(t_k)\Big[R_1M - v_z(t_k)L_1\frac{\mathrm{d}M}{\mathrm{d}z}\Big] - u(t_k)M + i_2(t_k)\times$$
$$\times\Big[v_z(t_k)M\frac{\mathrm{d}M}{\mathrm{d}z} - R_2L_1\Big]\Big\}, \quad (4)$$

where $u(t_k) = U_m\sin(\omega t_k + \psi_u)$; $\Delta t = t_{k+1} - t_k$;
$R_1 = R_1(T_1)$; $R_2 = R_2(T_2)$; $M = M(z)$;

$$\alpha_{1,2} = \pm\Bigg\{\frac{\Big(L_1R_2 + L_2R_1 - 2Mv_z\frac{\mathrm{d}M}{\mathrm{d}z}\Big)^2}{4\big(L_1L_2 - M^2\big)^2} - \frac{R_1R_2 - v_z^2\Big(\frac{\mathrm{d}M}{\mathrm{d}z}\Big)^2}{L_1L_2 - M^2}\Bigg\} +$$
$$+\frac{Mv_z\frac{\mathrm{d}M}{\mathrm{d}z} - L_1R_2 - L_2R_1}{2\big(L_1L_2 - M^2\big)}.$$

The magnitude of the anchor displacement together with the connected load relative to the inductor can be represented in the form of a recurrence relation [33]:

$$h_z(t_{k+1}) = h_z(t_k) + v_z(t_k)\Delta t + \vartheta\cdot\Delta t^2/(m_a + m_2), \quad (5)$$

where $v_z(t_{k+1}) = v_z(t_k) + \vartheta\cdot\Delta t/(m_a + m_2)$ is the anchor speed together with load; $\vartheta = F_z(z,t) - 0{,}125\pi\gamma_a\beta_aD_{e2}^2v_z^2(t_k)$; $F_z(z,t) = i_1(t_k)i_2(t_k)\frac{\mathrm{d}M}{\mathrm{d}z}$ is the instantaneous value of the axial electrodynamic force acting on the anchor; $m_2$, $m_a$ – mass of the anchor and the attached load respectively; $h_z$ – magnitude of anchor displacement; $\gamma_a$ – density of the medium of movement; $\beta_a$ – drag coefficient; $D_{e2}$ – outside diameter of the attached load.

The temperature of the $n$-th active element can be described by the recurrence relation [35]:

$$T_n(t_{k+1}) = T_n(t_k)\chi + (1-\chi)\left[T_0 + 4\pi^{-2} i^2(t_k) \times \right.$$
$$\left. \times R_n(T_n)\alpha_{Tn}^{-1} D_{en}^{-1} H_n^{-1}\left(D_{en}^2 - D_{in}^2\right)^{-1}\right], \qquad (6)$$

where $\chi = \exp\left\{-0{,}25\Delta t D_{en}\alpha_{Tn} c_n^{-1}(T_n)\gamma_n^{-1}\right\}$; $D_{en}$, $D_{in}$ – the outer and inner diameters of the $n$-th active element, respectively; $\alpha_{Tn}$, $c_n$, $\gamma_n$ – heat transfer coefficient, heat capacity and density of the $n$-th element respectively.

To calculate MLIT we use the following algorithm of cyclic action. We divide the working process into a number of numerically small time intervals $\Delta t = t_{k+1} - t_k$, within which all values are considered constant. In each cycle, using the parameters calculated at time $t_k$, as initial values, we calculate the parameters at time $t_{k+1}$. In the calculation cycle, the values of currents $i_n$, temperatures $T_n$, resistances $R_n(T_n)$ of active elements, values of axial electrodynamic force $f_z(z,t)$, velocity $v_z$ and displacement $h_z$ of the anchor, mutual inductance $M(z)$ between active elements are successively calculated.

To determine the currents on a numerically small calculation time interval $\Delta t$, we use linear equations with constant parameter values. We select the value of the calculation step $\Delta t$ in such a way that it does not have a significant effect on the calculation results, while ensuring the necessary accuracy.

Initial conditions of the mathematical model: $i_n(0)=0$; $T_n(0)=T_0$ – current and temperature of the $n$-th active element, respectively; $h_z(0)=h_{z0}$ – distance between active elements; $v_z(0)=0$ – armature speed along the $z$-axis; $u(0) = U_m \sin\psi_u$ – voltage of the alternating current source.

**Main parameters of MLIT.** Let us consider the electromechanical processes when starting magnetic levitation of the induction type, in which the inductor ($n$=1) and anchor ($n$=2) are made in the form of multi-turn disk windings. The active elements (inductor and anchor) are tightly wound with copper wire of diameter $d_0$=0.9 mm. Their outer diameter $D_{en}$=100 mm, and inner diameter $D_{in}$ =4 mm. The inductor has an axial height $H_1$=10 mm and contains turns $w_1$=480.

The active elements are made in the form of massive disks by impregnation and subsequent hardening of epoxy resin. They are installed horizontally and coaxially so that the initial distance between them $h_{z0}$=1 mm. The amplitude of the AC source voltage $U_m$ =100 V. The mass of the load connected to the anchor is $m_a$ =0.5 kg.

Let us consider the influence of the anchor parameters and the frequency of the AC source $f$ on the electromechanical processes that occur in the MLIT when the inductor is connected to the source. As anchor parameters we will use the number of turns $w_2$ and the axial height $H_2$. The change in the number of turns of the anchor $w_2$ is carried out layer by layer, which proportionally changes its height $H_2$.

Let us consider electromechanical processes when using an anchor with the following parameters: number of turns $w_2$=240, height $H_2$=5 mm. Figure 1 shows the starting electromechanical characteristics of the MLIT at the initial interval of 0.1 s when an alternating voltage with a frequency of $f$=50 Hz is applied to the inductor. In this case, the anchor with the connected load makes a vertical jump from the initial position. The instantaneous values of the source voltage $u$, the current density in the inductor $j_1$ and anchor $j_2$, the axial force $F_z$, the vertical velocity $v_z$ and the displacement $h_z$ of the anchor are presented as characteristics.

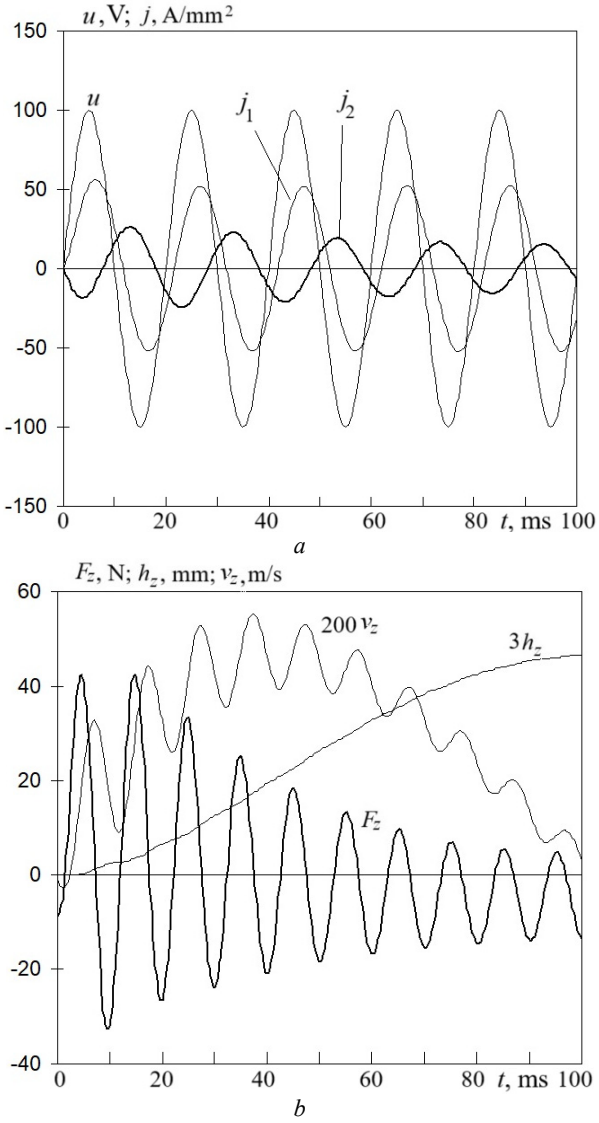


Fig. 1. Starting electromechanical characteristics of MLIT at source frequency $f$=50 Hz over a short interval

The inductor current lags in phase with the source voltage, which is explained by the active-inductive nature of the inductor resistance. However, the phase delay of the induced anchor current with respect to the inductor current is more important, since due to this, at certain moments, the currents flow in one direction, which leads to the emergence of a braking electrodynamic force directed downwards. Note that the total force providing vertical movement of the anchor $F_z$ also takes into account the gravity of the anchor and the load, as well as the aerodynamic resistance during movement.

As a result, the force $F_z$, due to the electrodynamic component acting on the anchor, has an alternating character with the positive component directed upwards predominating. It should be noted that the effect of the occurrence of the alternating nature of the electrodynamic force acting on the moving anchor when an alternating

voltage is applied to the inductor was first described in the works of Ukrainian scientists in 1986 [36].

This character of the electrodynamic force causes the pulsations of the anchor speed $v_z$. When the anchor with the load moves vertically relative to the inductor by a distance $h_z$, the induction current of the anchor and the positive component of the force acting on it decrease. In this case, the force of gravity begins to prevail, as a result of which the anchor begins to descend. The resulting oscillatory damping mechanical process can be seen in Fig. 2.

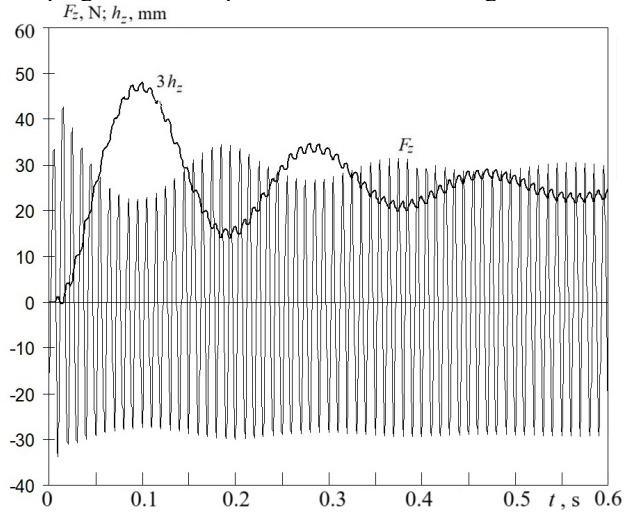


Fig. 2. Starting electromechanical characteristics of MLIT at source frequency $f$=50 Hz over an extended interval

When the anchor moves away from the inductor by a distance $h_z$, the upward component of the force $F_z$ decreases, and when the anchor approaches the inductor, this force increases. Since when the anchor moves upward, the electrodynamic force and the force of gravity are directed oppositely, and when it falls, they are directed in agreement, the downward force $F_z$ changes to a lesser extent than the force directed upward.

Such an oscillatory electromechanical process occurs with an increase in the oscillation period and a decrease in its amplitude. The first oscillation period is 0.17 s, the second – 0.2 s, etc. The greatest jump of the anchor with the attached load occurs initially to a height of $h_z$=15.9 mm, after which it drops to $h_z$=4.6 mm. Then the oscillation amplitude decreases and after about 1.0 s the oscillatory process practically fades out and the anchor with the attached load begins to stably levitate at a height of $h_z^*$=8.6 mm relative to the inductor.

When the inductor is connected to an alternating voltage source with a frequency of $f$ =100 Hz, the electromechanical processes change as follows (Fig. 3). The current density in the inductor $j_1$ decreases, which is explained by an increase in the inductor resistance, and the current density in the anchor $j_2$ increases, which is explained by an increase in the frequency of the magnetic field from the inductor.

As a result, the maximum electrodynamic force, and therefore the resulting lifting force $F_z$ increases, which causes the first jump of the anchor to a greater height $h_z$=22.7 mm. The period of mechanical oscillations is practically the same as when connecting the inductor to a voltage source with a frequency $f$=50 Hz, but with a greater amplitude.

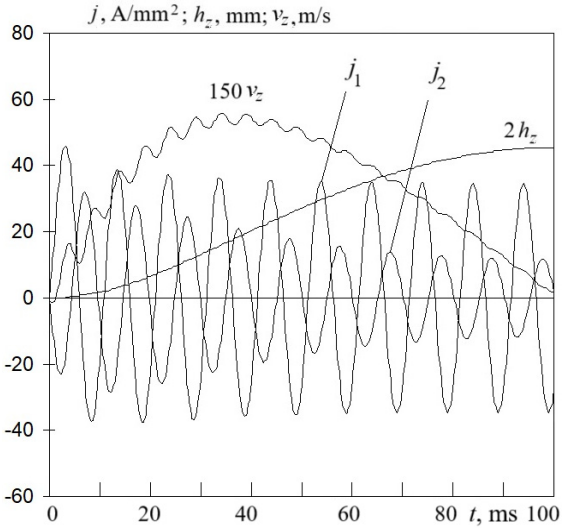


Fig. 3. Starting electromechanical characteristics of MLIT at source frequency $f$=100 Hz over a short interval

The higher the anchor bounce, the smaller the value of the induced current in the anchor $j_2$, and hence the value of the lifting force $F_z$ (Fig. 4). Depending on the value of the anchor bounce relative to the inductor, the induced current in the anchor changes to a greater extent than in the inductor, and the electrodynamic force to an even greater extent. After approximately 1.0 s, the anchor together with the load levitate at a steady height $h_z^*$=11 mm relative to the inductor.

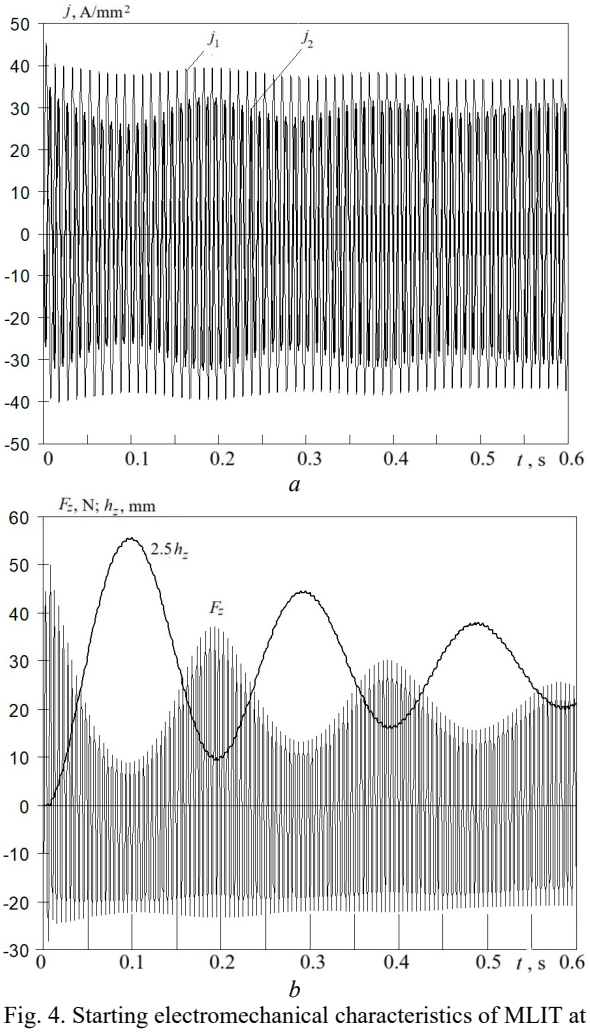


Fig. 4. Starting electromechanical characteristics of MLIT at source frequency $f$=100 Hz over an extended interval

The electromechanical parameters of the MLIT depend significantly on the anchor parameters and the frequency of the AC source voltage.

Figure 5 shows the maximum values of the current density in the inductor $j_{1m}$ and anchor $j_{2m}$, the force $F_{zm}$ and the steady-state height of anchor levitation with load $h_z^*$ depending on the frequency of the source voltage $f$. These dependencies are constructed for different anchor parameters: the number of turns $w_2$ and the corresponding height $H_2$. Since the turns are laid in layers, then, for example, at $w_2$=120, $H_2$=2.5 mm, at $w_2$=600, $H_2$=12.5 mm. In this case, the anchor mass also naturally changes.

With increasing source frequency $f$, the maximum current density in the inductor $j_{1m}$ decreases due to increasing inductive resistance. Moreover, the more turns in the anchor $w_2$, the greater the value of $j_{1m}$ due to the inductive effect of the anchor on the inductor.

With increasing source frequency $f$, the maximum current density in the anchor $j_{2m}$ changes ambiguously. This is due to two factors: increasing the frequency increases the EMF in the anchor, but the reduced inductor current excites a magnetic field of a smaller magnitude. In the range from 50 Hz, the value of $j_{2m}$ increases to a certain value, and then decreases with increasing frequency to 300 Hz. The fewer turns in the anchor, the higher the specified effect occurs at the higher source frequency.

This explains the nature of the change in the maximum force $F_{zm}$, which has the greatest value at a frequency in the range of 75–125 Hz. The more turns of the armature winding $w_2$, the greater the value of $F_{zm}$ and is achieved at a lower frequency. After the specified maximum value, the maximum force $F_{zm}$ decreases, and there is no obvious dependence on the number of turns $w_2$.

The dependence of the steady-state height $h_z^*$ of levitation of the anchor with a load on the frequency of the current in the inductor is to a certain extent similar to the dependence of the force on the frequency $F_{zm}(f)$, but with the peculiarity that with an increase in the number of turns of the anchor $w_2$, its mass also increases. The greatest levitation height $h_z^*$=15 mm is realized for the anchor $w_2$=480 s at a frequency of $f \sim$ 75 Hz.

That is, this anchor is made the same as the inductor. Note that at a frequency of 50 Hz, the anchor with the number of turns $w_2$=120 and an attached load will not levitate relative to the inductor at all.

It should be noted that the induction method of maintaining magnetic levitation in a stable mode is quite energy-consuming and significantly depends on the frequency of the supply voltage. Thus, for MLIT with the parameters considered above, when using an anchor with $w_2$=120 at $f$=50 Hz, the power of the power source is $P$ = 1.45 kW, and at $f$ = 300 Hz $P$ = 0.47 kW.

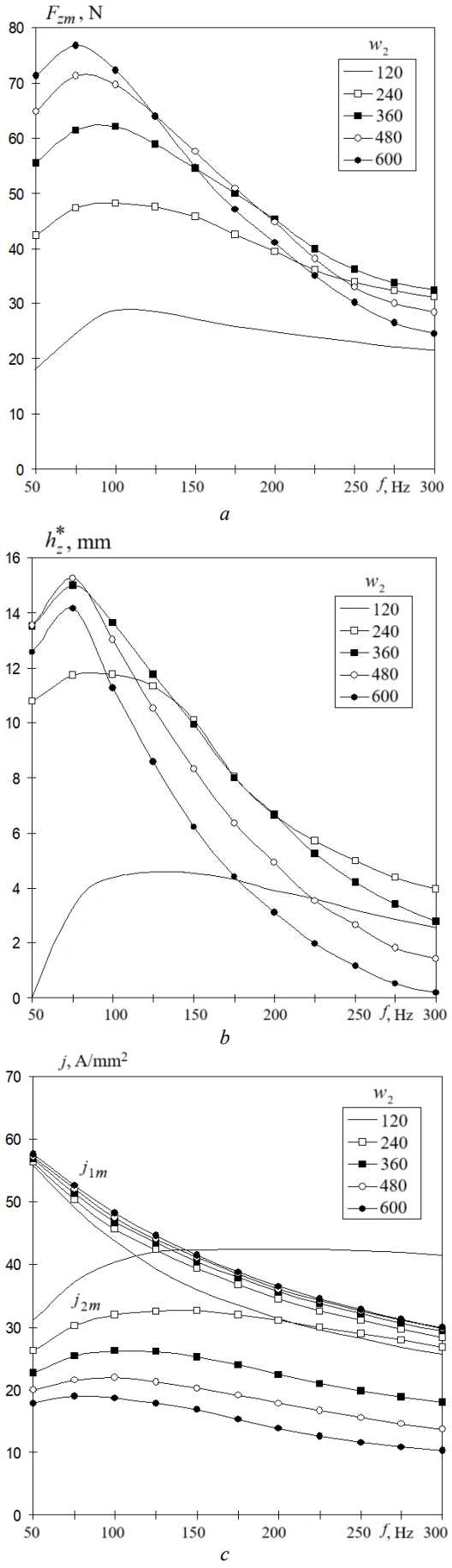


Fig. 5. Dependences of the electromechanical indicators of the MLIT on the frequency of the source voltage

To check the basic relationships, experimental studies of the MLIT were conducted in the laboratory of the General Electrical Engineering Department of NTU «KhPI». Figure 6 shows the initial position of the anchor, made in the form of an aluminum disk ring, relative to the inductor and the state of its stable levitation with an attached load (a roll of scotch tape). A plastic guide tube is used for strictly vertical movement of the anchor. Calculations performed for this installation using the proposed mathematical model coincided with the experimental data with an accuracy of 10 %.

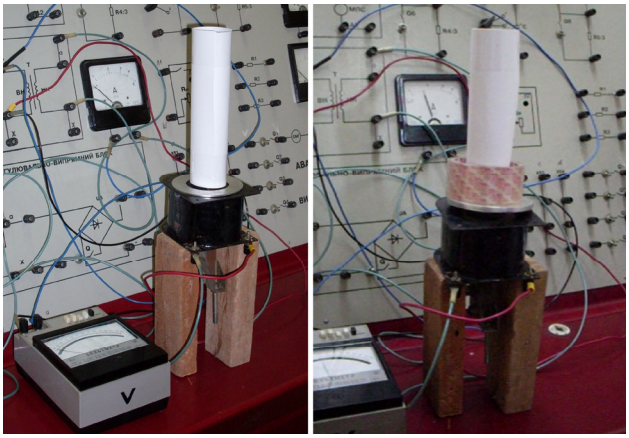

*a* *b*

Fig. 6. Experimental setup for studying MLIT in the initial (*a*) and working (*b*) state

The proposed magnetic levitation has a wide range of applications. For example, in high-precision gravimeters, in the vacuum chamber of which the optical angular reflector of the measuring system of the Michelson laser interferometer is freely moved in the gravitational field of the Earth, it can reduce autoseismic oscillations. Due to this, it is possible to increase the performance of the ballistic gravimeter with a symmetrical measurement scheme, which is the state primary standard of the unit of acceleration of free fall (National Scientific Center «Institute of Metrology», Kharkiv) [37].

**Conclusions.**

1. An analysis of magnetic levitation systems and their practical implementation is carried out, and the advantages of induction levitation are shown.

2. A mathematical model of magnetic levitation of the induction type with concentrated parameters of the inductor and anchor, represents solutions of equations describing interconnected electrical, magnetic, mechanical and thermal processes, in a recurrent form.

3. The influence of the frequency of the alternating current source on the electromechanical processes that occur when starting magnetic levitation of the induction type with different parameters of a multi-turn short-circuited anchor has been established.

4. When magnetic levitation is started, an oscillatory electromechanical process occurs, which is established after approximately 1 s. The highest established levitation height is realized for an anchor similar to an inductor, at a frequency of 75 Hz.

5. The results of experimental studies on the levitation of an aluminum disk with an attached load coincided with the calculated results obtained using the proposed mathematical model with an accuracy of 10 %.

**Conflict of interest.** The author declares no conflicts of interest.

REFERENCES

***1.*** Han H.-S., Kim D.-S. *Magnetic Levitation. Maglev Technology and Applications*. Springer Publ., 2016. 247 p. doi https://doi.org/10.1007/978-94-017-7524-3.

***2.*** Ramirez-Neria M., Gonzalez-Sierra J., Garcia-Antonio J.L., Garcia-Antonio J.A., Ramirez-Neria E. On the Sliding Mode Control of a Magnetic Levitation System Case: Thomson's Jumping Ring. *Proceedings of the International Conference of Control, Dynamic Systems, and Robotics*, 2014, paper no. 105. 8 p.

***3.*** Poletkin K.V., Asadollahbaik A., Kampmann R., Korvink J.G. Levitating Micro-Actuators: A Review. *Actuators*, 2018, vol. 7, no. 2, art. no. 17. doi: https://doi.org/10.3390/act7020017.

***4.*** Carneiro P., Soares dos Santos M.P., Rodrigues A., Ferreira J.A.F., Simões J.A.O., Marques A.T., Kholkin A.L. Electromagnetic energy harvesting using magnetic levitation architectures: A review. *Applied Energy*, 2020, vol. 260, art. no. 114191. doi: https://doi.org/10.1016/j.apenergy.2019.114191.

***5.*** Poletkin K. On the Static Pull-In of Tilting Actuation in Electromagnetically Levitating Hybrid Micro-Actuator: Theory and Experiment. *Actuators*, 2021, vol. 10, no. 10, art. no. 256. doi: https://doi.org/10.3390/act10100256.

***6.*** Zhou B., Dai C., Liu Z., Yu J., Liu H., Zhang B. Design and optimization of H-type asymmetric magnetic suspension vibration absorber for ships. *Journal of Vibration and Control*, 2025, vol. 31, no. 3–4, pp. 344-354. doi: https://doi.org/10.1177/10775463241226840.

***7.*** Liao H., Yuan H., Xie J. High-Precision Composite Control of Driving Current for Non-Contact Annular Electromagnetic Stabilized Spacecraft Subject to Multiple Disturbances. *Aerospace*, 2024, vol. 11, no. 8, art. no. 627. doi: https://doi.org/10.3390/aerospace11080627.

***8.*** Han W., Cai Y., Han W., Yin Z., Yu C. Review on Active Vibration Control Method of Magnetically Suspended System. *IEEE Access*, 2023, vol. 11, pp. 108117-108125. doi: https://doi.org/10.1109/ACCESS.2023.3317333.

***9.*** Fang J., Zheng S., Han B. Attitude Sensing and Dynamic Decoupling Based on Active Magnetic Bearing of MSDGCMG. *IEEE Transactions on Instrumentation and Measurement*, 2012, vol. 61, no. 2, pp. 338-348. doi: https://doi.org/10.1109/TIM.2011.2164289.

***10.*** Cai Y., Yu C., Ren Y., Wang W., Yin Z., Xia C. High Precision Attitude-Rate Measurement of Magnetically Suspended Control and Sensing Gyroscope Using Variational Mode Decomposition and Wavelet Transform. *IEEE Sensors Journal*, 2022, vol. 22, no. 2, pp. 1188-1198. doi: https://doi.org/10.1109/JSEN.2021.3131994.

***11.*** Dai C., Liu Z., Wang Y., Lin X., Liu H., Zhou B. Design and Optimization of a New Type of Magnetic Suspension Vibration Absorber for Marine Engineering. *Journal of Marine Science and Engineering*, 2023, vol. 11, no. 11, art. no. 2070. doi: https://doi.org/10.3390/jmse11112070.

***12.*** Li A.J., Zhou B.M., Jiang C.D., Liu D.Z., Wang E.H. Frequency-doubling displacement disturbance suppression of active magnetic bearing based on repetitive control. *2024 IEEE 10th International Power Electronics and Motion Control Conference (IPEMC2024-ECCE Asia)*, 2024, pp. 707-711. doi: https://doi.org/10.1109/IPEMC-ECCEAsia60879.2024.10567916.

***13.*** Cao S., Niu P., Wang W., Zhao T., Liu Q., Bai J., Sheng S. Novel Magnetic Suspension Platform with Three Types of Magnetic Bearings for Mass Transfer. *Energies*, 2022, vol. 15, no. 15, art. no. 5691. doi: https://doi.org/10.3390/en15155691.

***14.*** Bolyukh V.F., Vinnichenko A.I. Concept of an Induction-Dynamic Catapult for a Ballistic Laser Gravimeter.

*Measurement Techniques*, 2014, vol. 56, no. 10, pp. 1098-1104. doi: https://doi.org/10.1007/s11018-014-0337-z.
***15.*** Bolyukh V.F., Omel'chenko A.V., Vinnichenko A.I. Effect of Self-Seismic Oscillations of the Foundation on the Readout of a Ballistic Gravimeter with an Induction-Dynamic Catapult. *Measurement Techniques*, 2015, vol. 58, no. 2, pp. 137-142. doi: https://doi.org/10.1007/s11018-015-0675-5.
***16.*** Shearwood C., Ho K.Y., Williams, C.B., Gong H. Development of a levitated micromotor for application as a gyroscope. *Sensors and Actuators A: Physical*, 2000, vol. 83, no. 1–3, pp. 85-92. doi: https://doi.org/10.1016/S0924-4247(00)00292-2.
***17.*** Hatakenaka K., Hijikata W., Fujiwara T., Ohuchi K., Inoue Y. Prevention of thrombus formation in blood pump by mechanical circular orbital excitation of impeller in magnetically levitated centrifugal pump. *Artificial Organs*, 2023, vol. 47, no. 2, pp. 425-431. doi: https://doi.org/10.1111/aor.14443.
***18.*** Tang J., Li C., Zhou J., Wu Z. Effects of mechanical interfaces on magnetic levitation systems and analysis of self-excited vibration mechanisms in coupled systems. *Science China Technological Sciences*, 2024, vol. 67, no. 12, pp. 3925-3939. doi: https://doi.org/10.1007/s11431-024-2776-8.
***19.*** Shi H., Deng Z., Ke Z., Li Z., Zhang W. Linear permanent magnet electrodynamic suspension system: Dynamic characteristics, magnetic-mechanical coupling and filed test. *Measurement*, 2024, vol. 225, art. no. 113960. doi: https://doi.org/10.1016/j.measurement.2023.113960.
***20.*** Wang X.G., Liu Q., Zhang Y.J., Chen H.H. Research on Characteristic of Electromagnetic Force of Magnetic Suspension Device with Large Air-Gap. *Applied Mechanics and Materials*, 2013, vol. 401-403, pp. 239-244. doi: https://doi.org/10.4028/www.scientific.net/AMM.401-403.239.
***21.*** Abd. Aziz P.D., Li Q., Rodriguez E., Deng Z. A Preliminary Study on Electromagnetic Levitation Design Topology. *2020 IEEE International Conference on Applied Superconductivity and Electromagnetic Devices (ASEMD)*, 2020, pp. 1-2. doi: https://doi.org/10.1109/ASEMD49065.2020.9276251.
***22.*** Bolyukh V.F., Shchukin I.S. Improving the Efficiency of a Linear Pulse Electromechanical Accelerator Due to Excitation by a Series of Pulses. *2020 IEEE KhPI Week on Advanced Technology (KhPIWeek)*, 2020, pp. 205-210. doi: https://doi.org/10.1109/KhPIWeek51551.2020.9250077.
***23.*** Bolyukh V.F. Effect of electric conducting element on indicators of linear pulse electromechanical converter induction type. *Technical Electrodynamics*, 2020, no. 3, pp. 22-29. doi: https://doi.org/10.15407/techned2020.03.022.
***24.*** Skubov D.Y., Indeitsev D.A., Udalov P.P., Popov I.A., Lukin A.V., Poletkin K.V. Nonlinear Dynamics of a Micromechanical Non-Contact Induction Suspension. *Mechanics of Solids*, 2023, vol. 58, no. 6, pp. 2011-2023. doi: https://doi.org/10.3103/S0025654423600307.
***25.*** Rahman A., Mizuno T., Takasaki M., Ishino Y. An Equivalent Circuit Analysis and Suspension Characteristics of AC Magnetic Suspension Using Magnetic Resonant Coupling. *Actuators*, 2020, vol. 9, no. 3, art. no. 52. doi: https://doi.org/10.3390/act9030052.
***26.*** Jeffery R.N., Amiri F. Thomson's Jumping Ring Over a Long Coil. *The Physics Teacher*, 2018, vol. 56, no. 3, pp. 176-180. doi: https://doi.org/10.1119/1.5025301.
***27.*** Tjossem P.J.H., Cornejo V. Measurements and mechanisms of Thomson's jumping ring. *American Journal of Physics*, 2000, vol. 68, no. 3, pp. 238-244. doi: https://doi.org/10.1119/1.19407.
***28.*** Donoso G., Ladera C.L. The naked toy model of a jumping ring. *European Journal of Physics*, 2014, vol. 35, no. 1, art. no. 015002. doi: https://doi.org/10.1088/0143-0807/35/1/015002.
***29.*** Ng C. The Thomson Jumping Ring Experiment and Ideal Transformer. *The Physics Teacher*, 2022, vol. 60, no. 5, pp. 376-379. doi: https://doi.org/10.1119/5.0036490.
***30.*** Ladera C.L., Donoso G. Unveiling the physics of the Thomson jumping ring. *American Journal of Physics*, 2015, vol. 83, no. 4, pp. 341-348. doi: https://doi.org/10.1119/1.4902891.
***31.*** Tjossem P.J.H., Brost E.C. Optimizing Thomson's jumping ring. *American Journal of Physics*, 2011, vol. 79, no. 4, pp. 353-358. doi: https://doi.org/10.1119/1.3531946.
***32.*** Taweepong J., Thamaphat K., Limsuwan S. Jumping ring experiment: effect of temperature, non-magnetic material and applied current on the jump height. *Procedia Engineering*, 2012, vol. 32, pp. 982-988. doi: https://doi.org/10.1016/j.proeng.2012.02.042.
***33.*** Bolyukh V.F., Shchukin I.S. Influence of an excitation source on the power indicators of a linear pulse electromechanical converter of induction type. *Technical Electrodynamics*, 2021, no. 3, pp. 28-36. doi: https://doi.org/10.15407/techned2021.03.028.
***34.*** Bolyukh V.F., Katkov I.I. Influence of the Form of Pulse of Excitation on the Speed and Power Parameters of the Linear Pulse Electromechanical Converter of the Induction Type. *Proceedings of the ASME 2019 International Mechanical Engineering Congress and Exposition. Volume 2B: Advanced Manufacturing*, 2019, V02BT02A047. doi: https://doi.org/10.1115/IMECE2019-10388.
***35.*** Bolyukh V.F., Kashansky Y.V., Schukin I.S. Features of excitation of a linear electromechanical converter of induction type from an AC source. *Electrical Engineering & Electromechanics*, 2021, no. 1, pp. 3-9. doi: https://doi.org/10.20998/2074-272X.2021.1.01.
***36.*** Vaskovsky Yu.M., Chemeris V.T., Petrovsky V.P., Shats A.N. Physical modeling of the features of anchor acceleration in a pulse electromechanical converter of induction type. *Technical Electrodynamics*, 1986, no. 3, pp. 66-69.
***37.*** Bolyukh V., Vinnichenko O., Neyezhmakov P., Omelchenko A. Reduction of auto seismic oscillations of the ballistic laser gravimeter on account of the excitation of the induction-dynamic catapult by a pulse packet. *Ukrainian Metrological Journal*, 2020, no. 3, pp. 3-11. doi: https://doi.org/10.24027/2306-7039.3.2020.216765.

*Received 13.12.2024*
*Accepted 02.02.2025*
*Published 02.05.2025*

*V.F. Bolyukh* [1]*, Doctor of Technical Science, Professor,*
[1] National Technical University «Kharkiv Polytechnic Institute», 2, Kyrpychova Str., Kharkiv, 61002, Ukraine,
e-mail: vfbolyukh@gmail.com (Corresponding Author)

*How to cite this article:*
Bolyukh V.F. Electromechanical processes during the start of induction-type magnetic levitation. *Electrical Engineering & Electromechanics*, 2025, no. 3, pp. 3-10. doi: https://doi.org/10.20998/2074-272X.2025.3.01